

Short communication

Alkali hexatitanates— $A_2Ti_6O_{13}$ ($A = Na, K$) as host structure for reversible lithium insertion

R. Dominko^{a,c,*}, L. Dupont^{b,c}, M. Gaberšček^{a,c}, J. Jamnik^{a,c}, E. Baudrin^{b,c}

^a National Institute of Chemistry, P.O.B. 660, SI-1001 Ljubljana, Slovenia

^b Laboratoire de Réactivité et Chimie des Solides, UMR CNRS 6007, 33 rue Saint Leu 80039, Amiens Cedex, France

^c Advanced Lithium Energy Storage Systems (ALISTORE) Network of Excellence, Slovenia

Available online 30 June 2007

Abstract

Electrochemical lithium insertion into two isostructural titanium-based oxides, $K_2Ti_6O_{13}$ and $Na_2Ti_6O_{13}$ has been investigated. Although the two compounds differ mainly from their particle size and cell volume, pronounced differences in the insertion mechanism have been evidenced. They can accommodate about three Li per formula unit at relatively low potentials (1.5–0.9 V versus Li reference), which qualifies them as potential alternatives to $Li_4Ti_5O_{12}$. The main limitations are their rate capabilities and capacity retention related to large particles and parasitic electrolyte decomposition, respectively.

© 2007 Elsevier B.V. All rights reserved.

Keywords: $Na_2Ti_6O_{13}$; $K_2Ti_6O_{13}$; Titanium oxide; Lithium insertion; Li-ion batteries

1. Introduction

Exhaustion of fossil fuel became a perspective which will surely drive the search for new energy sources and/or the use of renewable energies. For most of the alternatives (photovoltaic, wind energy, etc.), such an evolution will be only credible if highly performing storage systems are developed. Among the possibilities, Li-ion batteries represent a serious candidate in term of volumetric and specific energy density. Besides the improvement of battery engineering and management, the choice of electrode materials is one of the key parameters. Alloying and conversion reactions are nowadays largely investigated as alternative commercial negative electrodes. However classical intercalation reactions still lead to interesting systems. For instance, $Li_4Ti_5O_{12}$ is now one of the best candidates because of its “zero strain” lithium insertion process leading to a reversible capacity of 150–160 mAh g⁻¹ at 1.5 V versus Li^+/Li^0 [1–3]. Among the very rich structural family of titanium-based oxides, anatase [4], rutile [5–7] and $TiO_2[B]$ [8], were also reported with quite good electrochemical properties for nanosized materials. For bulk materials, such oxides can reversibly accommodate about 0.5 lithium ions per titanium atoms. However, e.g., using

nano-particles, the capacity can be increased up to nearly 1 mol of lithium per transition metal [9,10]. Another quite common characteristic of titanium-based oxides is their electrochemical activity within the potential range from 2 V to 1 V versus Li^+/Li^0 depending on the host structure. For instance, reduction of Ti^{4+} to Ti^{3+} in an octahedral oxygen environment typically occurs at a potential between 1.8 V and 1.6 V. Surprisingly, among various existing alkali element-based titanium oxides with favourable structures for lithium insertion, only $Li_4Ti_5O_{12}$ and $Li_2Ti_3O_7$ [11,12] have been reported as electrode materials. Recently we moved on the study of a sodium hexatitanate, namely $Na_2Ti_6O_{13}$ [13]. Contrary to our expectations, the presence of sodium in the pristine material is not detrimental to the electrochemical properties and in fact effectively seems to stabilize the structure during the insertion/deinsertion process. Lithium can be reversibly inserted at low voltage (between 1 V and 1.5 V) with a capacity of 150 mAh g⁻¹ at C/3. Furthermore, as far as we know, this is the lowest voltage range reported for the insertion into a titanium-based oxide.

In this contribution we report on the microstructural characterisation and electrochemical properties of a material which is isostructural to $Na_2Ti_6O_{13}$, namely potassium hexatitanate ($K_2Ti_6O_{13}$), which can also accommodate lithium at such low voltages. The electrochemical properties and the structural evolution during lithium insertion will be described and discussed in relation with the sodium hexatitanate $Na_2Ti_6O_{13}$.

* Corresponding author at: National Institute of Chemistry, P.O.B. 660, SI-1001 Ljubljana, Slovenia. Tel.: +386 14760362; fax: +386 14760422.

E-mail address: Robert.Dominko@ki.si (R. Dominko).

Table 1
Refined lattice parameters of $A_2Ti_6O_{13}$ ($A = Na, K$)

Phase	a (Å)	b (Å)	c (Å)	β (°)
$Na_2Ti_6O_{13}$	15.0949(2)	3.7452(8)	9.1693(5)	99.01(1)
$K_2Ti_6O_{13}$	15.597(4)	3.7972(5)	9.110(2)	99.80(1)

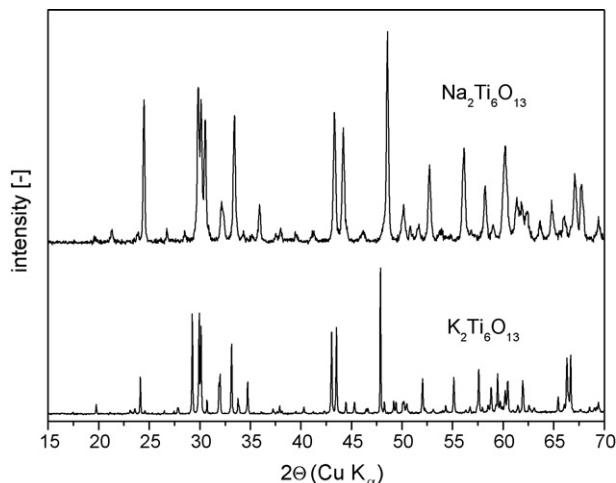


Fig. 1. XRD patterns of the prepared $Na_2Ti_6O_{13}$ and $K_2Ti_6O_{13}$ phases.

2. Experimental

Well crystalline $K_2Ti_6O_{13}$ samples were obtained by solid-state reaction of anatase particles with KOH in slight excess

(about 10 mol%). The precursors were grinded manually in a mortar for 20 min and calcined in air at 800 °C for 10 h. $Na_2Ti_6O_{13}$ sample was prepared from a thermal treatment of protonated sodium titanate hydrate (Na,H)-Ti-O nanotubes as previously described [13].

Electrochemical characterisation was performed on electrodes prepared by casting and pressing a mixture of 85 wt.% of active material, 7 wt.% of teflon binder (Aldrich 44,509/6) and 8 wt.% of carbon black (Printex XE2, Degussa) on a copper foil. Prior to the test this 0.5 cm² surface area electrode, loaded with about 5 mg/cm², was dried under vacuum at 120 °C for 24 h for comparison, different electrolyte composition were used: 1 M LiPF₆ in EC:DMC (1:1 ratio by weight), 1 M LiPF₆ in EC:PC (1:1 ratio by volume) and 1 M LiClO₄ in PC.

A laboratory-made three-electrode test cell was used to carry out the electrochemical tests. The working and the counter (lithium) electrodes were held apart with two separators (Celgard No. 2402) between which a thin lithium strip reference electrode was positioned. The cells were assembled in an argon-filled glove box at room temperature. Charge–discharge curves and cycling voltammograms were recorded using a VMP3 (Biologic Co. Claix, France) potentiostat/galvanostat at room temperature in galvanostatic modes and cyclic voltammetry (0.02 mV s⁻¹). The cut-off voltages were set to 3 V/1 V and 3 V/0.9 V versus Li⁺/Li⁰ for $Na_2Ti_6O_{13}$ and $K_2Ti_6O_{13}$, respectively.

The morphology and texture were evaluated using a scanning electron microscope (SEM, Supra 35LV) and a high-resolution transmission electron microscope with a FEI TECNAI F20

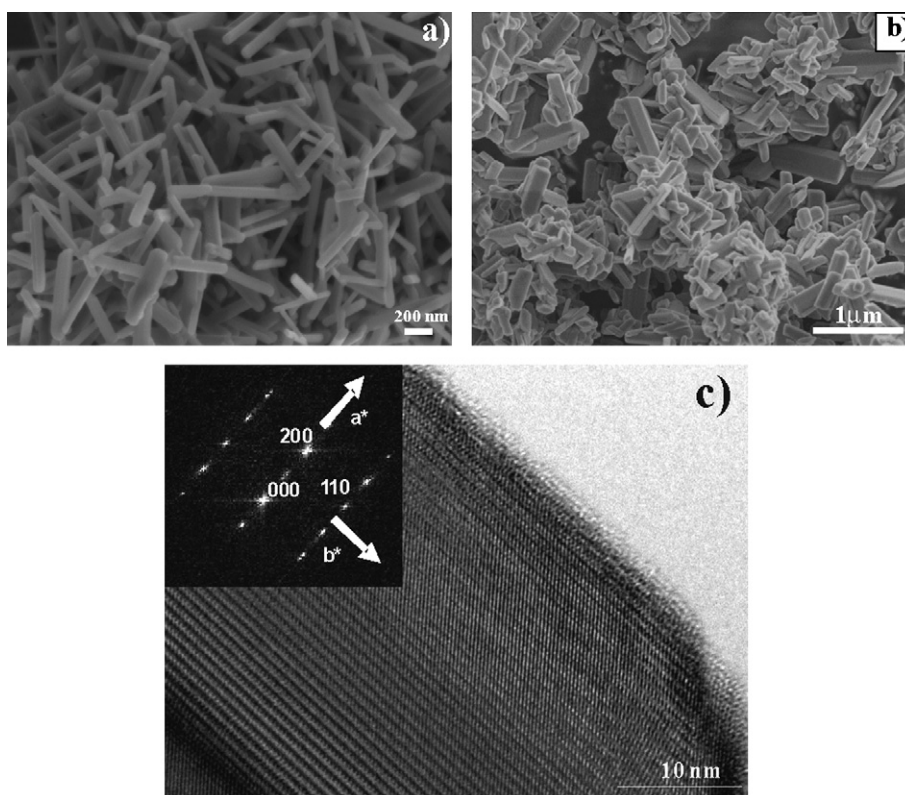


Fig. 2. SEM micrographs of (a) $Na_2Ti_6O_{13}$ and (b) $K_2Ti_6O_{13}$ particles; (c) HRTEM micrograph of a $Na_2Ti_6O_{13}$ particle along the [001] zone axis.

microscope. In situ X-ray measurements were obtained in a laboratory-made cell controlled by a Macpile automatic cycling/data recording system (Biologic SA, Claix, France) and using a Bruker D8 diffractometer (Co K α).

3. Results and discussion

The sodium hexatitanate (Na₂Ti₆O₁₃) was obtained by dehydration at 800 °C of the protonated sodium titanate (Na,H)-Ti-O nanotubes formed by hydrothermal treatment of a suspension of TiO₂ in 10 M NaOH [13]. A pure phase is clearly obtained with refined cell parameters (space group *C2/m*) in agreement with previous reports (Table 1) [14]. On the other hand, the potassium hexatitanate (K₂Ti₆O₁₃) was prepared by a solid-state process at the same final temperature (800 °C) in air. Sharper X-ray diffraction peaks are observed indicating that larger crystallite sizes are formed. Again, all the peaks were indexed in the space group *C2/m* [15] with noteworthy larger cell parameters as compared to the sodium hexatitanate (Fig. 1).

The structure of these materials is formed from corrugated chains of three edge sharing octahedra assembled in such a way to form 3 × 1 tunnels along *c*-axis. The alkali ions are located into these tunnels. The main increases in the *a* and *b* param-

eters thus results from the larger size of potassium compared to sodium ion. Moreover, this highly anisotropic structure, induced the formation of rod-like particles (Fig. 2a). We can notice a better homogeneity (in size and morphology) for the sodium-containing sample and smaller particles compared to K₂Ti₆O₁₃ (Fig. 2b). This illustrates once more the greatest ability to control particle size and morphology by using soft chemistry methods than ceramic reactions. To determine the orientation of the particle, we performed HRTEM. The obtained pictures and electron diffraction patterns (Fig. 2c) indicated surprisingly that the crystals are growing preferentially along the *b*-direction, that is, perpendicular to the tunnels direction.

While these two materials are close in term of structure and texture, we observe some differences in their electrochemical and structural evolution. As underlined in the introduction, a common feature is their capability to accommodate lithium in the potential range 0.9–1.5 V versus Li⁺/Li⁰ as observed from cyclic voltammetry (Fig. 3a) and galvanostatic experiments (Fig. 3b). While for Na₂Ti₆O₁₃ two stages are observed (the absence of additional phenomenon was checked down to 0.8 V), the K₂Ti₆O₁₃ analogue exhibits three energetically dif-

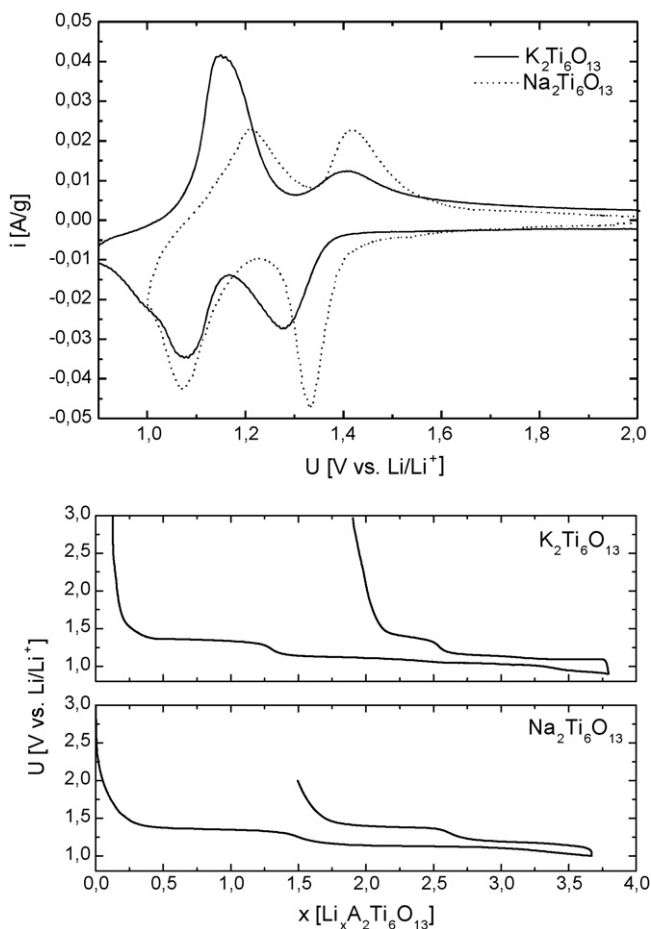


Fig. 3. Cycling voltammetry and galvanostatic curves of the first cycle for sodium and potassium hexatitanates. Galvanostatic curves were obtained at current density corresponding to insertion of 1 mol of lithium in 10 h.

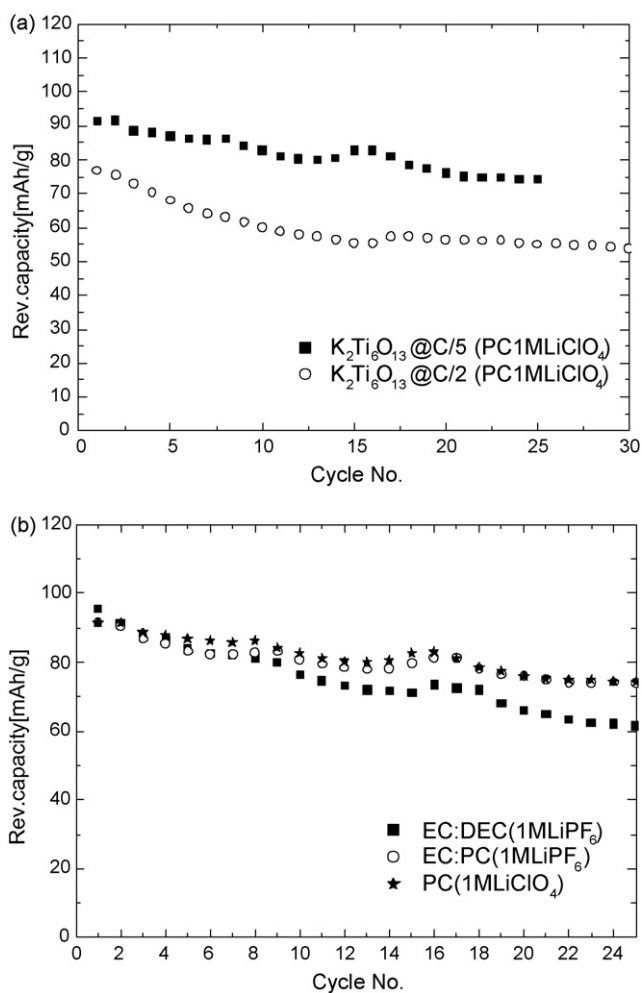


Fig. 4. (a) Capacity retention for the insertion of lithium into K₂Ti₆O₁₃ at different current densities (*C/n* correspond to the insertion of 1 mol of lithium in *n* hours) and (b) as a function of cycle numbers in the different electrolyte compositions at *C/5* rate (between 0.9 V and 3 V vs. Li⁺/Li⁰).

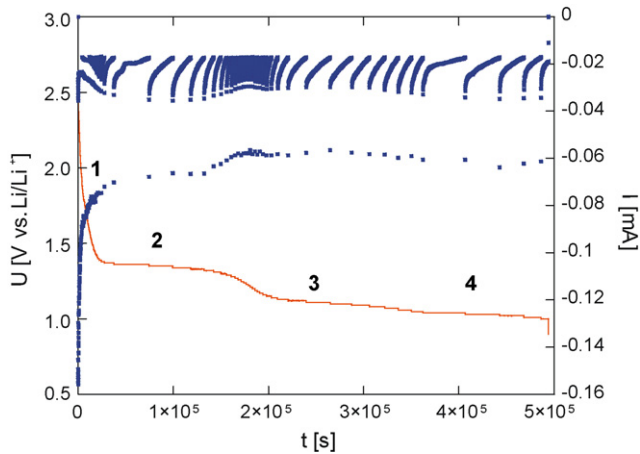


Fig. 5. PITT measurements (with $|I_{lim}| = C/60$ and steps of 10 mV) of lithium insertion into $K_2Ti_6O_{13}$ phase.

ferent stages together with an initial solid solution type voltage decrease. Slightly more than three lithium ions can be inserted into these two materials, corresponding to capacities of about 150 mAh g^{-1} . This is comparable to the capacity of the popular $Li_4Ti_5O_{12}$ material [2]. In a previous report, we showed that for $Na_2Ti_6O_{13}$, the irreversible capacity observed from the electrochemical curves was related to some side reactions with the electrolyte since the reaction was structurally highly reversible [13]. Such irreversibility is also obtained for $K_2Ti_6O_{13}$ in the present work.

At moderate current densities, the amount of lithium ion reversibly inserted decreases considerably, namely, to 2 Li at $C/5$ and 1.5 Li at $C/2$ (Fig. 4a). At this point, we have to emphasize again that $A_2Ti_6O_{13}$ ($A = Na, K$) phases are formed from rod-like shape particles with b -axis running along the longest dimension. As the channels also run perpendicular in this direction, the solid state transport should not be hindered and thus the limited rate capabilities probably results from the presence of potassium ions within the tunnels. Similarly to $Na_2Ti_6O_{13}$ phase [13], we found that the main capacity fading comes from the electrochemical phenomena occurring at the lowest potential (around 0.9–1.2 V), consistent with a possible SEI formation around these voltages. However, it seems from tests in different electrolytes that the capacity fading is slightly lowered using PC based electrolytes (Fig. 4b). Further experiments are underway to coat such materials with a uniform carbon coating trying to reduce such effects [16].

To get a further insight in the insertion/deinsertion mechanism of $K_2Ti_6O_{13}$, we performed potentiostatic intermittent titration technique (PITT) and in situ X-ray diffraction measurements during the first reduction.

The voltage evolution observed during the PITT experiment confirms the presence of four steps during the lithium insertion into $K_2Ti_6O_{13}$ (Fig. 5). While the first and third phenomena seemed to be related to solid solutions domains, the bell-shape like current evolution for steps 2 and 4 are clearly linked to the presence of biphasic transitions. This has been confirmed by in situ X-ray diffraction measurements. From the pristine

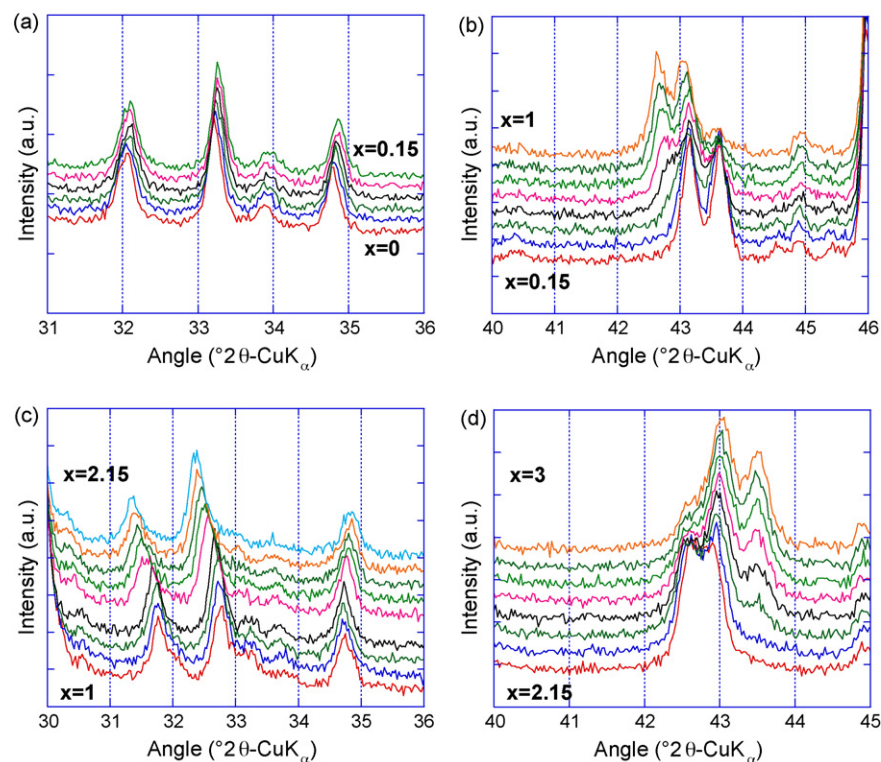


Fig. 6. Selected XRD patterns obtained during the first reduction of $K_2Ti_6O_{13}$ vs. lithium: (a) solid solution during insertion of 0.15 mol of lithium per formula unit; (b) first biphasic transition leading to final composition of $Li_{\approx 1}K_2Ti_6O_{13}$ followed by (c) solid solution formation to composition of approximately $Li_{\approx 2.15}K_2Ti_6O_{13}$ in (d) second biphasic transition leading to final composition of $Li_{\approx 3}K_2Ti_6O_{13}$.

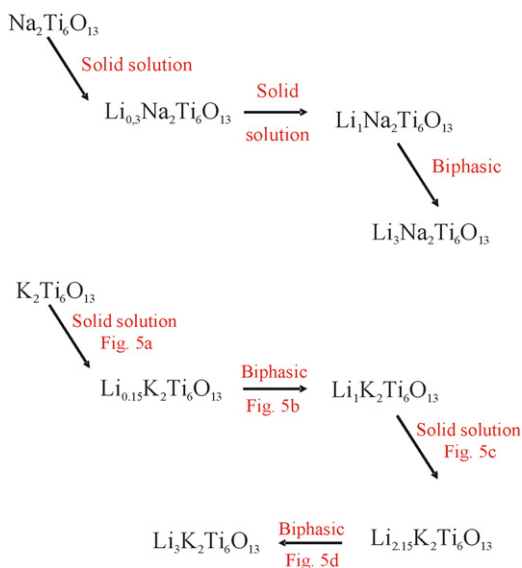


Fig. 7. A scheme of the structural changes during lithium insertion into $\text{Na}_2\text{Ti}_6\text{O}_{13}$ and $\text{K}_2\text{Ti}_6\text{O}_{13}$ phase.

material to a composition $x=0.15$, a continuous shift of Bragg reflections towards higher angle values is noticed (Fig. 6a) and responsible for the voltage decrease from O.C.V. to about 1.4 V. Further lithium insertion produces a pseudo-plateau at 1.3 V (step 2), leading to a composition $\text{Li}_{\approx 1}\text{K}_2\text{Ti}_6\text{O}_{13}$. During this step, we observe the appearance of new reflections confirming the biphasic transition (Fig. 6b). This finding reveals the first important difference in behaviour for the two $\text{A}_2\text{Ti}_6\text{O}_{13}$ structures. Indeed, in the case of $\text{Na}_2\text{Ti}_6\text{O}_{13}$ the electrochemical pseudo-plateau at about 1.35 V (corresponding to formation of $\text{Li}_{\approx 1}\text{Na}_2\text{Ti}_6\text{O}_{13}$) was related to a solid solution evolution. Differences are also found at lower voltages (that is, at lithium content higher than $\text{Li}_{\approx 1}\text{A}_2\text{Ti}_6\text{O}_{13}$). While lithium insertion from the composition of $\text{Li}_{\approx 1}\text{Na}_2\text{Ti}_6\text{O}_{13}$ up to the final $\text{Li}_{\approx 3}\text{Na}_2\text{Ti}_6\text{O}_{13}$ proceeds through a single biphasic transition [13], two different mechanisms are evidenced for the potassium hexatitanate. From $\text{Li}_{\approx 1}\text{K}_2\text{Ti}_6\text{O}_{13}$ to approximately $\text{Li}_{\approx 2.15}\text{K}_2\text{Ti}_6\text{O}_{13}$, a solid solution is observed causing the increase of cell volume as seen from Fig. 6c. Again, further lithium insertion induces the appearance of a biphasic transition finished around $\text{Li}_{\approx 3}\text{K}_2\text{Ti}_6\text{O}_{13}$ (Fig. 6d). This final composition corresponds to a new phase $\text{Li}_3\text{K}_2\text{Ti}_6\text{O}_{13}$ (Fig. 6). For easier comparison, schemes of the structural evolution for $\text{Na}_2\text{Ti}_6\text{O}_{13}$ and $\text{K}_2\text{Ti}_6\text{O}_{13}$ have been summarized in Fig. 7.

The two main differences for the materials presented in this work are the particle size and the different cell volumes related to the larger potassium ion as compared to sodium. From previous work, it is possible that the extension of the solid solution domains up to a composition $\text{Li}_{\approx 1}\text{A}_2\text{Ti}_6\text{O}_{13}$ for the sodium-based compound is related to the small crystallite size. Indeed, in the case of titania (anatase [17] or rutile [7]), we showed such evolution as the crystallite sized decreased and proposed a relation with capability of nanosized particle to expand (particle breathing) to reduce the strains. On the other hand, the impossibility to accommodate such strain in larger particle or on further lithium insertion (higher than a limit composition) would

induce biphasic transitions. Discussion on the insertion mechanism beyond this $x=1$ composition is difficult at the present time and further measurements are requested to determine the structures of the formed phase $\text{Li}_{\approx 1}\text{K}_2\text{Ti}_6\text{O}_{13}$

4. Conclusions

In this paper, we report on the insertion of lithium into potassium hexatitanate, $\text{K}_2\text{Ti}_6\text{O}_{13}$, in the potential range between 1.5 V and 0.9 V versus metallic lithium. The insertion behaviour is compared to the sodium analogue ($\text{Na}_2\text{Ti}_6\text{O}_{13}$). Despite the fact that both structures are more or less identical, the lithium insertion into $\text{K}_2\text{Ti}_6\text{O}_{13}$ phase proceeds through four steps (during which two new phases have been evidenced) while $\text{Na}_2\text{Ti}_6\text{O}_{13}$ accommodates better the lithium up to $x=1$ after which a biphasic transition is noticed. Lithium insertion into both structures is remarkably reversible with a maximum 3 mol of lithium accommodated per formula unit, corresponding to a capacity of about 150 mAh g^{-1} . The low operating voltages observed make this family of alkali-based hexatitanates viable as alternative to $\text{Li}_4\text{Ti}_5\text{O}_{12}$ as anode material if we are able to improve the capacity retention and rate capabilities.

Acknowledgements

The financial support from the Ministry of Education, Science and Sport of Slovenia and the support from the European Network of Excellence 'ALISTORE' network are acknowledged.

References

- [1] M.M. Thackeray, J. Electrochem. Soc. 142 (1995) 2558.
- [2] E. Ferg, R.J. Gummow, A. de Kock, M.M. Thackeray, J. Electrochem. Soc. 141 (1994) L147.
- [3] G.G. Amatucci, F. Badway, A. Du Pasquier, T. Zheng, J. Electrochem. Soc. 148 (2001) A930.
- [4] T. Ohzuku, T. Kodama, T. Hirai, J. Power Sources 14 (1985) 153.
- [5] Y.-S. Hu, L. Kienle, Y.-G. Guo, J. Maier, Adv. Mater. 18 (2006) 1421.
- [6] M.A. Reddy, M.S. Kishore, V. Pralong, V. Caignaert, U.V. Varadaraju, B. Raveau, Electrochem. Commun. 8 (2006) 1299.
- [7] E. Baudrin, S. Cassaignon, M. Koelsch, J.-P. Jolivet, J.-M. Tarascon, Electrochem. Commun. 9 (2007) 337.
- [8] A.R. Armstrong, G. Armstrong, J. Canales, R. Garcia, P.G. Bruce, Adv. Mater. 17 (7) (2005) 862.
- [9] A.R. Armstrong, G. Armstrong, J. Canales, P.G. Bruce, Angew. Chem. Int. Ed. 43 (2004) 2286.
- [10] M. Wagemaker, W. Borghols, F. Mulder, Abstract 237, IMLB 2006 Meeting, Biarritz, France.
- [11] R.K.B. Gover, J.R. Tolchard, H. Tukamoto, T. Murai, J.T.S. Irvine, J. Electrochem. Soc. 146 (1999) 4348.
- [12] M.E. Arroyo y de Dompablo, A. Varez, F. Garcia-Alvarado, J. Solid State Chem. 153 (2000) 132.
- [13] R. Dominko, E. Baudrin, P. Umek, D. Arcon, M. Gaberscek, J. Jamnik, Electrochem. Commun. 8 (2006) 673.
- [14] S. Andersson, A.D. Wadsley, Acta Crystallogr. 15 (1962) 194.
- [15] K. Byrappa, S. Gali, B.M.R. Wanklyn, A.B. Kulkarni, S.K. Patil, G. Narendranath, J. Mater. Sci. Lett. 9 (1990) 898.
- [16] R. Dominko, M. Gaberscek, M. Bele, D. Mihailovic, J. Jamnik, Eur. Ceram. Soc. 27 (2007) 909.
- [17] G. Sudant, E. Baudrin, D. Larcher, J.-M. Tarascon, J. Mater. Chem. 15 (2005) 1263.